Avoidance of Neoclassical Tearing Mode Locking and Disruption by Feedback-Induced Accelerating Electro-Magnetic Torque

M. Okabayashi[1], E.J. Strait[2], A.M. Garofalo[2], J.M. Hanson[3], Y. In[4], R.J. La Haye[2], D. Shiraki[3], and F. Volpe[3]

[1]*Princeton Plasma Physics Laboratory, Princeton, New Jersey 08543-0451, USA.*
[2]*General Atomics, PO Box 85608, San Diego, California 9186-5608, USA.*
[3]*Columbia University, New York, New York 10027, USA*
[4]*FAR-TECH, Inc., 10350 Science Center Dr., San Diego, California 92121-1136, USA*

Disruptions by macro MHD instabilities such as resistive wall mode (RWM) and neoclassical tearing mode (NTM) are considered to be one of the most substantial roadblocks to achieving safe steady-state operation of tokamak-based fusion reactors. Over the last few years, RWM suppression and its control have been explored by various groups. Magnetic control of tearing mode and locking avoidance were initiated more than two decades ago [1] and have received revived attention recently in combination with electron cyclotron current drive [2]. Recently serious concerns on ITER operational limit have revived the interest in this subject. Here, by using applied non-axisymmetric fields optimized for n=1 RWM feedback control [3], we explored the avoidance of NTM locking and associated disruption. The fundamental process is the introduction of the electro-magnetic (EM) JxB torque caused by the toroidal phase shift between the externally-applied n=1 field and the excited NTM fields. This injected EM torque compensates the mode momentum loss due to the electromagnetic braking by the finite amplitude of NTM and its interaction with the resistive wall (Fig. 1). The fine control of the toroidal phase of the applied external field relative to the NTM is provided by the feedback system.

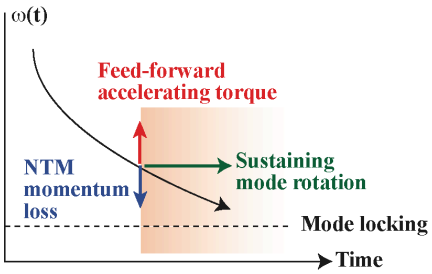

Fig. 1. The schematic diagram of NTM locking avoidance with feedback.

The requested n=1 helical field pattern and feedback parameters are similar to those in standard RWM feedback operation except that the requested coil field is shifted toroidally in a feed-forward manner so that finite phase difference is always imposed, regardless of the time evolution of the mode structure and plasma configuration (Fig. 2). With this approach, in case the RWM becomes marginally unstable, the system can function simultaneously to reduce the resonance field amplification. Although the finite phase shift is provided by the feed-forward feedback logic, the overall total phase shift is determined by the closed-loop system including the plasma response to the applied field. As discussed later, the feedback process functioned with the phase of NTM δB_p in-phase with the applied feedback $B_{r.ext}$. This phase relation produces near maximum torque for the given mode amplitude and coil current. This favorable nonlinear process seems to make the locking avoidance more resilient to the unexpected evolution of the disruption onset. The feedback stability is analyzed with a cylindrical model to map the marginal condition.

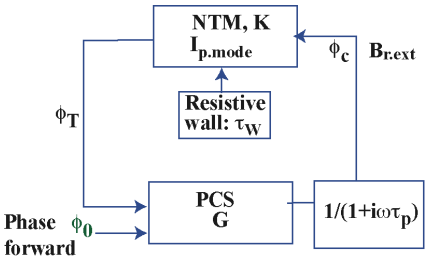

Fig. 2. Feedback schematic diagram including the wall stabilizing effects.

1. Introduction

The application of EM torque on the NTM can be studied with a model analogous to that of a synchronous rigid motor model. Here, the NTM mode rotation is on the plasma frame namely,

$$I\frac{d}{dt}\omega = I\frac{\omega}{\tau_{loss}} - T\,\mathrm{Im}\left\{B_{r.ext} * I_{p.modes}\right\} \quad , \qquad \omega = \frac{d}{dt}\,\phi \quad , \tag{1}$$

where I is the moment of inertia of the mode, and τ_{loss} the total mode momentum loss including the coupling to the bulk plasma and the momentum input from neutral beam injection (NBI), T represents the coefficient for maximum torque JxB with applied feedback field $B_{r.ext}$ and the effective poloidal mode current $I_{p.mode}$. The schematic of the overall feedback is shown in Fig. 2, where K is the NTM response to the applied n=1 field, τ_p the filtering time constant in the feedback logic and ϕ_0 is the preset toroidal phase shift in feedback between the observed toroidal phase and the applied n=1 field. Steady-state constant frequency condition, d/dt=0, yields

Since the NTM response is unknown, we assume absolute value of K is unity with the phase shift ϕ_m. The total phase shift is expressed $\phi_T = \phi_m + \phi_0$. Steady-state constant frequency condition, d/dt=0, yields

$$\frac{\omega}{\tau_{loss}} - (T/I)\,\mathrm{Im}\left\{B_{r.ext} * I_{p.modes}\right\} = 0 \quad , \tag{2}$$

where the frequency ω_0 is the steady-state frequency. When $\omega_0 \sim 0$, the mode rotation frequency is given by

$$\frac{\omega_0}{\tau_{loss}} \sim (T/I) * |KG| * I^2_{p.mode}\,\sin\Delta\phi_T \quad . \tag{3}$$

In standard RWM feedback operation, the phase of feedback coil current is set to produce the $B_{r.ext}$ phase for compensating δB_r of the mode. Since the δB_r is shifted toroidally by $\pi/2$ from the δB_p, the applied $B_{r.ext}$ does not produce the EM torque in the standard RWM feedback. Here, the phase shift $\Delta\phi_T$ is defined as $\Delta\phi_T$ = (phase difference between $B_{r.ext}$ and δB_p - $\pi/2$). With this definition, $\Delta\phi_T$=0 corresponds to the standard RWM feedback operation and the phases of maximum positive/negative torque are expressed by $\Delta\phi_T = \pm\pi/2$. Equation (2) predicts that switching of the mode direction occurs with switching of the polarity of $\Delta\phi_T$.

2. Experimental Observations

An example of NTM locking avoidance is shown in Fig. 3. The plasma conditions for the onset of NTM are normalized plasma beta $\beta_N \sim 2.5$ and the plasma rotation velocity around q=2 is ~50 km/s corresponding to 8 kHz. Coils used for the feedback are the two internal coil arrays (I-coils) located above/ below the midplane [3]. The filtering parameter, τ_p, was 40 ms and the toroidal phase offset, ϕ_0, was set to -30 deg. The NTM started to grow around 2500 ms. At the NTM onset, the mode rotation frequency (not shown) and bulk plasma rotation were reduced in a synchronized manner due to the increase of interaction between NTM and the wall. The feedback started to become effective when the rotation frequency approached toward the inverse of the filter time constant $1/\tau_p$ (~20 Hz). The plasma rotation around the q~2 surface became nearly zero presumably due to the large amplitude NTM viscous effects. The frequency was sustained at ~20 Hz over several energy confinement times with the mode amplitude of 20 Gauss. T_i profile evolution (by charge exchange recombination spectroscopy measurement) showed the large magnetic island width ~10 cm. β_N dropped from 2.5 to 1.5 and was then sustained at that value with the

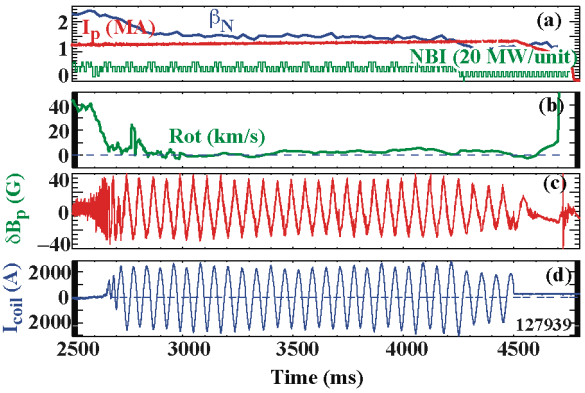

Fig. 3. Feedback performance of the NTM locking avoidance (#127939), (a) plasma current, β_N, NBI power, (b) plasma rotation at q~2 surface, (c) a sensor signal, and (d) a feedback coil current.

~10 MW NBI input power. The NTM amplitude [Fig. 3(c)] decreased with lower NBI power at 4000 ms, consistently with NTM physics understanding.

The transient process by the feedback termination leading to disruption is shown in Fig. 4. Before the coil current was turned off at t = 4500 ms, the toroidal phase shift of sensor signals [Fig. 4(b)] at four toroidal locations show that the mode rotation was sustained by the applied external field. The termination of feedback caused the rapid reversal of rotation direction, indicating that the mode moment of inertia is small. The mode survived ~200 ms with very slow rotation and locking occurred at 4700 ms leading to disruption. The fact that the disruption occurred shortly after turning the feedback off clearly indicates the advantage of feedback-driven mode rotation.

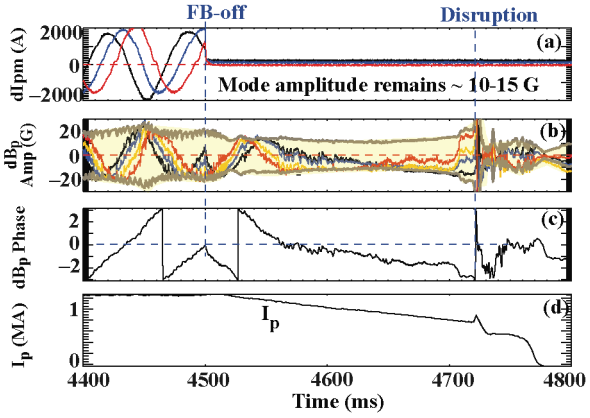

Fig. 4. The disruption after the feedback termination, (a) the feedback currents, (b) the four sensor signals, (c) the toroidal phase and (d) the plasma current (#127939).

Phase relation between the mode δB_p and the applied $B_{r.ext}$ is documented in Fig. 5. In Fig. 5(b), the solid black line is for the phase of current maximum, the dotted line is for that of current minimum and the blue line is the mode δB_p. The nearly-in-phase between the mode δB_p and the $B_{r.ext}$ can produce the maximum torque for the given coil current and mode amplitude. When the phase polarity, ϕ_0, was shifted from -30 deg to +30 deg at 3375 ms, the mode direction was reversed. The δB_p phase change was 180 degs out of phase relative to the $B_{r.ext}$ [Fig. 4(d)] as predicted from switching the mode direction. The phase relation remains producing nearly-maximum torque. The transient time period ~10 ms, was comparable to the filtering time constant, τ_p, rather than the bulk plasma parameters such as momentum confinement time.

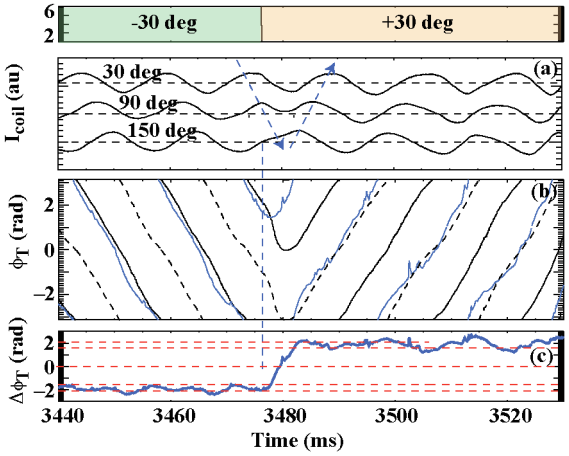

Fig. 5. The phase difference of the external field and the mode (#139605) (a) feedback coil currents at 30, 90 and 150 deg, (b) the toroidal phase of applied field $B_{r.ext}$ and NTM δB_p: the black line represents the $B_{r.ext}$ phase and the blue line for NTM δB_p phase, and (c) the phase difference $\Delta\phi_T$ between the $B_{r.ext}$ and δB_p mode. The dotted lines correspond to $\phi_T = \pm\pi/2\ \pm\pi/6$.

3. Marginal Stability

Here, advantage of feedback-driven mode rotation control is discussed using a simple cylindrical model, which defines the process with a rigid mode rotating with $\exp(i\omega t)$ [4]. By assuming the momentum loss $\omega/\tau_{loss} \sim$ zero in Eq. (2), the torque balance condition yields, $A(\omega)=(T/I)(f/g) = 0$,

$$f = -(\omega\tau_p)^3(\tau_w/\tau_p) - (\omega\tau_p)(\tau_w/\tau_p) + G\sin(\phi_0)\left[1-(\omega\tau_p)^2(\tau_w/\tau_p)\right] - G\cos(\phi_0)(\omega\tau_p)\left[1+(\tau_w/\tau_p)\right] \quad , \qquad (4)$$

$$g = \left[1+(\omega\tau_p)^2\right]\left[1+(\omega\tau_p)^2(\tau_w/\tau_p)^2\right] \quad , \qquad (5)$$

where ϕ_0 is the pre-set value of forward phase shift shown in the feedback schematic (Fig. 2). With this assumption, the EM momentum input is dissipated by the interaction between the NTM and the resistive wall although the interaction process itself could involve complex processes depending upon the details of the plasma properties. The condition $f(\omega)=0$ provides

the torque balance equilibrium condition. It should be noted that Eqns (4,5) remain intact by switching of polarities of $\phi_0 \rightarrow -\phi_0$ together with $\omega \rightarrow -\omega$. Thus, the offset phase shift ϕ_0 determines the mode direction in this model, as was with the experimental observations.

Stability characteristics are shown in Fig. 6. The dotted curves are without preset ($\phi_0=0^o$) the red solid curves correspond to $\phi_0=30^o$ preset phase shift and the blue curves are for $\phi_0=30^o$ shift corresponding to one unstable and one stable branch of the cubic-ω Eq. (4). For no phase shift, $\phi_0=0^o$, [Fig. 6(a)] with high gain, $|G|>>|G_{crit}|= \{(\tau_w/\tau_p)/[1+(\tau_w/\tau_p)]\}$, the system can approach finite frequency $\omega\tau_p \sim [G^*(\tau_p/\tau_w)]^{1/2}$, and consequently finite $\omega\tau_p$ such as ~2 produces considerable phase shift between the mode and the applied field [Fig. 6(c)], which is the crucial factor for avoiding locked mode appearance. Finite $\omega\tau_p \neq 0$ resulted in the increase of the stability depth of the torque balanced condition $df(\omega)/d\omega<0$ [equivalent to $dA(\omega)/d\omega<0$] [Fig. 6(b)]. The mode behavior with finite offset ϕ_0 at $\omega\tau_p=0$ needs further analysis. The parameters in the experiment are: (1) $\omega\tau_p=3.8$, $\omega\tau_w=1.1$ ($\tau_p/\tau_w=0.3$) and (2) $\omega\tau_p=5.0$ and $\omega\tau_w=0.38$ ($\tau_p/\tau_w=0.075$). Both cases were observed with the phase shift of 90–130 degrees, consistent with the model predictions when the normalized gain G is 5–6 (the model values are in the asymptotical range of normalized gain G in Fig. 6). This estimated normalized gain range is not much different from the one with other feedback applications such as RWM dynamic error field correction. The predictions of this cylindrical model are consistent with the main parameters such as mode rotation frequency, filtering time constant.

The remarkable consistency of this simple model and observations implies that the feedback-driven rotation control is a fundamental process dominated by a few identifiable parameters. Thus, model should be possible to apply for other devices like ITER. In the discussion above, the feedback-driven mode control has been discussed with a specific case. However, it was found that the process is more general, which will be discussed separately.

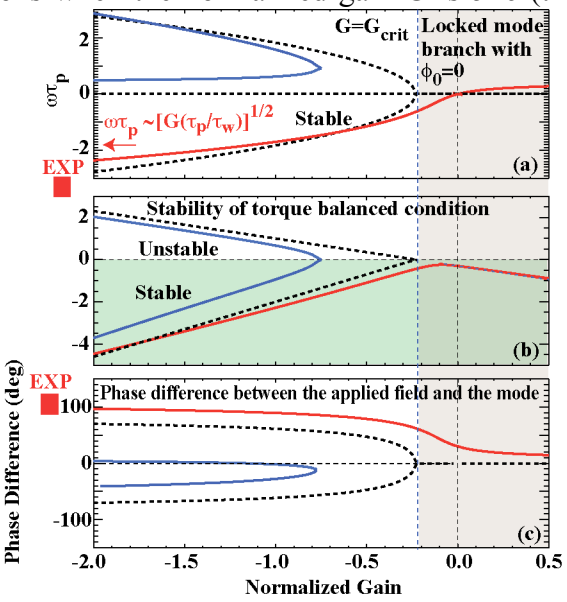

Fig. 6. The predictions by a cylindrical model: (a) the $\omega\tau_p$ dependence on gain, (b) the stability of torque balanced condition calculated with $df(\omega)/d\omega$, and (c) the phase difference between the applied field and the mode.

4. Summary

We have explored the avoidance of NTM locking and its associated disruption by applying non-axisymmetric magnetic fields regulated by a feedback system. The process involves the introduction of the EM JxB torque. The steady-state toroidal phase of the mode, δB_p, is found to be nearly in-phase with the feedback-supplied $B_{r.ext}$, producing near maximum torque for the given mode amplitude and the coil current. This phase relation makes the locking avoidance more resilient to disruptions. The simple model prediction is consistent with the experiments.

This work was supported by the US Department of Energy under DE-AC02-09CH11466, DE-FC02-04ER54609, DE-FG02-08ER85195, and DE-FG02-04ER54761.

[1] T. Hender et al., Nucl Fusion **32**, 2091 (1992).
[2] F. Volpe et al., Phys. Plasmas 16,102502 (2009)
[3] M. Okabayashi et al., Nucl. Fusion **45**, 1715 (2005).
[4] A.M. Garofalo et al., Phys. Plasmas **9**, 4573 (2002).